AGU PUBLICATIONS

JGR

Journal of Geophysical Research: Oceans

RESEARCH ARTICLE

10.1002/2014JC010134

Moored observations of synoptic and seasonal variability in the East Greenland Coastal Current

B. E. Harden[1], F. Straneo[1], and D. A. Sutherland[2]

[1]Woods Hole Oceanographic Institution, Massachusetts, USA, [2]Department of Geological Sciences, University of Oregon, Eugene, Oregon, USA

Key Points:
- Depth of Polar layer in EGCC exhibits significant synoptic variability
- Winds force much of the variability through downwelling
- Freshwater content increases through winter due to advection from upstream

Correspondence to:
B. E. Harden,
bharden@whoi.edu

Citation:
Harden, B. E., F. Straneo, and D. A. Sutherland (2014), Moored observations of synoptic and seasonal variability in the East Greenland Coastal Current, *J. Geophys. Res. Oceans*, *119*, 8838–8857, doi:10.1002/2014JC010134.

Received 8 MAY 2014
Accepted 1 DEC 2014
Accepted article online 8 DEC 2014
Published online 23 DEC 2014

Abstract We present a year-round assessment of the hydrographic variability within the East Greenland Coastal Current on the Greenland shelf from five synoptic crossings and 4 years of moored hydrographic data. From the five synoptic sections the current is observed as a robust, surface intensified flow with a total volume transport of 0.66 ± 0.18 Sv and a freshwater transport of 42 ± 12 mSv. The moorings showed heretofore unobserved variability in the abundance of Polar and Atlantic water masses in the current on synoptic scales. This is exhibited as large vertical displacement of isotherms (often greater than 100 m). Seasonally, the current is hemmed into the coast during the fall by a full depth Atlantic Water layer that has penetrated onto the inner shelf. The Polar Water layer in the current then thickens through the winter and spring seasons increasing the freshwater content in the current; the timing implies that this is probably driven by the seasonally varying export of freshwater from the Arctic and not the local runoff from Greenland. The measured synoptic variability is enhanced during the winter and spring period due to a lower halocline and a concurrent enhancement in the along-coast wind speed. The local winds force much of the high-frequency variability in a manner consistent with downwelling, but variability distinct from downwelling is also visible.

1. Introduction

In this paper, we present year-round, continuous measurements of hydrographic variability within the East Greenland Coastal Current (EGCC). Very little is currently known about the scales of variability in this current, but such knowledge is crucial for understanding how the ocean transports freshwater from the Arctic to the North Atlantic, and how the current forces circulation within Greenland's glacial fjords. We aim to explore features of the current that are pertinent to these processes.

The East Greenland Coastal Current is part of a wider boundary current system that exports significant quantities of freshwater and sea ice from the Arctic, sub-Arctic and Greenland ice sheet to the North Atlantic [*Rudels et al*., 2002; *Bacon et al*., 2002; *Dickson et al*., 2008]. It exists on the inner continental shelf of Greenland south of Denmark Strait and onshore of the shelf-break East Greenland Current (see Figure 1). The current is formed of a wedge of fresh Polar origin water that is banked against the Greenland coast onshore and atop Atlantic origin water, which has encroached onto the shelf. The resulting lateral density gradient (controlled primarily by salinity) supports the surface intensified velocity signature of the East Greenland Coastal Current. The buoyancy driven flow extends for much of the length of the Greenland shelf south of Denmark Strait with a width of 20–30 km [*Sutherland and Pickart*, 2008]. It was originally hypothesized as forming due to melt water runoff from the Greenland landmass [*Bacon et al*., 2002], but now, water mass properties indicate that it has closer ties to the East Greenland Current at the shelf-break, possibly branching inshore south of the Denmark Strait or further upstream [*Sutherland et al*., 2009].

What we currently understand about the current's dynamics and transport has been largely gleaned from measurements taken aboard research vessels and, as such, are clustered in the ice-free summer months [*Bacon et al*., 2002; *Wilkinson and Bacon*, 2005; *Sutherland and Pickart*, 2008; *Sutherland et al*., 2013]. At Cape Farewell, transport estimates have ranged from 0.8 to 2.0 Sv [*Bacon et al*., 2002; *Pickart et al*., 2005]. To the north along the wider part of the shelf, *Sutherland and Pickart* [2008] measured transports of 0.6–1.4 Sv, and *Bacon et al*. [2014] report a modeled summertime transport of 1.9 Sv (increasing to 3.8 Sv in the winter). *Wilkinson and Bacon* [2005] used geostrophic velocities from historical hydrography to show a range of

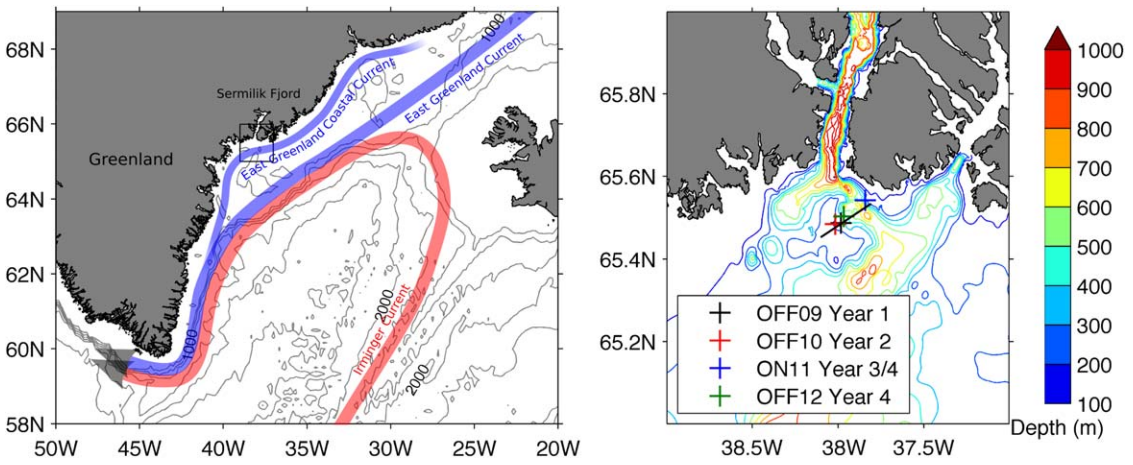

Figure 1. (left) Map of region showing the wider circulation of surface waters along the southeast coast of Greenland. Note, the precise origins of the East Greenland Coast Current have yet to be definitively shown. (right) Zoomed in plot of the field study region (from black box in left plot). Moorings are shown by colored crosses and the hydrographic section line is shown by a black line. Bathymetry is a combination of *Schjøth et al*. [2012], IBCAO v.3, and seal-derived data [*Sutherland et al*., 2013].

0.2–2.0 Sv (for the baroclinic component of the transport). The combined East Greenland Current system is thought to account for 2–3 Sv [*Pickart et al*., 2005] making the coastal current a significant part of the boundary current system.

Freshwater transport estimates in the East Greenland Coastal Current have ranged from 10 to 100 mSv [*Bacon et al*., 2002; *Wilkinson and Bacon*, 2005; *Sutherland and Pickart*, 2008]. The annual mean freshwater export out of the Arctic through Fram Strait is currently thought to be 66 mSv [*de Steur et al*., 2009] with an additional 70 mSv of sea ice export [*Kwok et al*., 2004]. Both transports are larger in the wintertime. Even with the small freshwater addition from the Greenland ice sheet en route (∼15 mSv) [*Bamber et al*., 2012], the East Greenland Coastal Current is clearly a significant contributor to the equatorward export of Arctic freshwater.

Some attempts have been made to explain the range of historic transports in the East Greenland Coastal Current. *Wilkinson and Bacon* [2005] argue that the transport is proportional to the maximum thickness of the Polar Water layer, which can vary significantly between crossings (of the order 100 m). *Sutherland and Pickart* [2008] argue for an acceleration in the current and an increase in transport due to along coast winds. They also show that the freshwater content of the current increases as it flows down the coast of Greenland, consistent with melt water input from Greenland and in situ sea ice melt.

The paucity of knowledge on the scales and forms of variability in the East Greenland Coastal Current is a major motivator for this study. We need to understand what variability is intrinsic to the system and how its hydrography evolves over the year if we are to effectively assess the role this current plays in delivering fresh water to the North Atlantic and how best to monitor it over the long term.

Variability in the current's hydrography may also play a role on the stability of the Greenland ice sheet by forcing warm Atlantic Water to enter Greenland's outlet fjords. Over the past decade Greenland has been losing mass from its ice sheet at an increasing rate [*Velicogna*, 2009]. A significant portion of this loss is due to acceleration of the outlet glaciers, particularly those along the southeast coast of Greenland [*Stearns and Hamilton*, 2007; *Howat et al*., 2007; *Moon et al*., 2012]. Ocean-ice interactions might be a significant driver of this acceleration [*Holland et al*., 2008; *Straneo and Heimbach*, 2013]; in many of Greenland's outlet fjords, significant quantities of warm Atlantic Waters have been found [*Straneo et al*., 2012], their presence providing a year-round mechanism for melting the glacial tongue and undercutting the grounding line [*Vieli and Nick*, 2011]. The hypothesis is that, if Atlantic Water has an efficient pathway from the open ocean to the tongues of Greenland's glaciers, then reported increases in North Atlantic water temperatures [*Myers et al*., 2007; *Bersch et al*., 2007; *Thierry et al*., 2008] can translate directly to increased melt rates on Greenland's glaciers and trigger ice sheet mass loss [*Murray et al*., 2010] (for a full review, see *Straneo and Heimbach* [2013]).

The precise details of the mechanisms by which these waters make their way from the open Atlantic Ocean to the head of fjords are currently poorly understood. It is possible that one part of this journey is regulated

Table 1. Overview of Mooring Data[a]

Period	Mooring	Latitude	Longitude	Instruments	Mean Depths (m)
Year 1 2009–2010	OFF09a	64.29°N	37.59°W	Microcat	221
				Thermistors	200, 180, 160, 150, 140, 130, 120
	OFF09b	65.30°N	37.58°W	Microcat	291
				Aquadopp	291
Year 2 2010–2011	OFF10	65.29°N	39.01°W	Microcat	252
				Thermistors	232, 212, 192, 182, 172, 162, 152
Year 3 2011–2012	ON11	65.33° N	37.50°W	RBR	301
				Thermistors	281, 261, 241, 221
Year 4 2012–2013	ON11 (cont)	65.33°N	37.50°W	RBR	301
	OFF12	65.30°N	37.58°W	Microcat	281

[a]Mooring locations, instrumentation and depths. All years of deployment ran from summer to summer, see text for turn around times. The instruments referred to in the table are: Microcat: SBE37SM; RBR: XR 420 CTD; Aquadopp: Nortek Aquadopp; Thermistors: Chain composed of ONSET tidbits and an RBR DR1050 depth recorder.

by the East Greenland Coastal Current. The southeast Greenland fjords have a two layer system similar to that seen on the shelf: Cold, fresh Polar Water overlaying warm, salty Atlantic Water [*Straneo et al.*, 2012]. This observation led to the hypothesis that the water properties in the fjord are being largely dictated by the shelf. One dominant exchange mechanism is due to horizontal density gradients between the shelf and the fjord. The fjord adjusts to any such gradient through the excitation of an inflow-outflow circulation in the fjord. This is called the intermediary circulation [*Klinck et al.*, 1981; *Stigebrandt*, 1990; *Nilsen et al.*, 2008] and may result in large lateral mixing and the replenishment of fjord's Polar and Atlantic layers with the properties of their shelf counterparts. Evidence of the intermediary circulation in Greenland fjords has been observed [*Straneo et al.*, 2010; *Jackson et al.*, 2014], but we currently know very little about and the scales of variability on the shelf or what forces them.

A more complete understanding of the scales of hydrographic variability in the East Greenland Coastal Current is important for assessing both fresh water transport along the Greenland shelf and investigating shelf-fjord exchange. Both process are key to the climate stability of the planet. In this paper we aim to shed light on these processes through the analysis of hydrographic data from the Ammassalik region of southeast Greenland outside the mouth of Sermilik fjord (Figure 1). In this region, a large trough cuts the shelf from the shelf-break to the fjord mouth. Near the shore, a small channel ($\sim$15 km) branches off from the main trough and passes the mouth of Sermilik Fjord. It is from within this channel that we present measurements, allowing us to assess variability in the East Greenland Coastal Current at a point right next to an instrumented outlet fjord. We will assess the variability from hydrographic sections and fixed moorings, and investigate the impact of along-coast winds in driving the changes seen.

2. Data

Sections of hydrographic properties across the channel outside Sermilik Fjord (see Figure 1 for location) were taken on multiple occupations of the same section on five cruises to the region. The sections for this study fell on the following days: 31 August 2008, 24 August 2009, 24 August 2011, 20 September 2012 and 18 August 2013. All shipboard data were gridded onto the same section (see Figure 1) using a Laplacian-spline interpolation scheme with a horizontal grid spacing of 1 km and vertical spacing of 5 m. Geostrophic velocities were calculated from this gridded product and referenced to detided Lowered Acoustic Doppler Current Profiler (LADCP) data over a depth range of 50–300 m. Tidal velocities for the LADCP data were estimated from a harmonic analysis (T-TIDE in Matlab) [*Pawlowicz et al.*, 2002] of 1 year of moored velocity data at OFF09b (see Table 1). These tidal current estimates compare well with predictions made with an Arctic Ocean inverse barotropic tidal model (AOTIM) [*Padman and Erofeeva*, 2004], and are generally small (e.g., $<$0.05 m s^{-1}) compared to the overall signal. For 2008, we have no LADCP data so we reference the geostrophic velocities to the mean LADCP section from the other 4 years. The bathymetry used for the sections is from an underway echosounder in 2009 [*Schjøth et al.*, 2012; *Sutherland et al.*, 2013].

Transports each year were calculated from the gridded sections. For freshwater transport estimates we chose a reference salinity of 34.8 psu to be able to make direct comparisons with *Sutherland and Pickart* [2008] who report the most comprehensive assessment of transports in the current. Higher values (34.9–34.95 psu)

have also been used historically [*Bacon et al*., 2002; *Wilkinson and Bacon*, 2005; *de Steur et al*., 2009], but result in only a ~3% change in our recorded transports.

The time evolving hydrographic properties on the inner shelf are characterized by data from a number of mooring deployments over a 4 year period (see Figure 1 for location and listed in Table 1). All the moorings had a CTD (see Table 1 for details) mounted near to the base of the mooring to measure temperature, salinity and pressure. Some moorings were also equipped with a string of thermistors stretching up approximately 100 m with varying resolution (see Table 1) to measure temperature profiles.

The moorings were placed on either the onshore or offshore side of the channel and we will therefore refer to them with the prefixes OFF and ON respectively, as in Table 1. The moorings were each deployed over 1 year (summer to summer) with the exception of ON11, which couldn't be recovered at the end of its initial deployment year and was subsequently left out for a further year before begin recovered—it recorded data for this entire period although the buoyancy in the thermistor string was lost during the attempted mooring recovery in 2012. Therefore the thermistor string is unusable for the second year that ON11 was deployed. The moorings were deployed and recovered at the same time that the synoptic sections were taken (see above for dates with the addition of 22 August 2010). For analysis, all data were despiked and interpolated to a 1 h resolution. In the 2009–2010 deployment year there were two moorings (OFF09a and OFF09b) separated by 2 km and a depth of 70 m. These produced very similar records, so for ease we averaged the CTD records and (unless otherwise stated) use this as the data from this deployment year and call this record OFF09 with a representative depth of 256 m for all analysis.

The moored CTDs were calibrated before deployment and after recovery. In addition, cross calibration with the ship-board hydrographic data provided a means of assessing any instrument drift. These were found to be negligible except for the salinity record of ON11, which showed a drift over the 2 years of deployment. In year 4, we could compare the record from ON11 with the concurrent record from OFF12 and correct for the drift based on comparing Θ-S properties. Through this method it became clear that most of the drift occurred in year 4. In year 3, when there was no contemporaneous time series to compare to, no correction was made.

A pressure recorder was mounted at the top of the thermistor string to record the depth of the top of record. Unfortunately, in the first two deployment years, these malfunctioned so we have no record of any blow-down of the moorings for these years. In the third deployment year, the pressure recorder worked and we only observed small ($<$10 m) and infrequent episodes of blowdown. We therefore use the nominal distance of the thermistors from the anchor to calculate their depths for all moorings.

We use the pressure record from the base of the mooring as a proxy for sea surface height (SSH). Even though the instrument is not bottom mounted (lying about 3 m from the bottom) and we have no way of categorically dismissing blowdown as a cause of pressure changes, we feel this is a valid method for three reasons. For one, the mooring configuration was such that the deep instrument was mounted beneath a large buoyant float that would have likely been able to keep the very short mooring taut during stronger current events. Second, in year three we observed that the bottom pressure sensor is not affected by blow-down of the top sensor (the records are not correlated during these times) showing that the blowdown of the thermistor string is decoupled from the lower mooring. And thirdly, the record from year 4 shows the same variability as those in years 1–3 that had the thermistor strings attached. If blow down accounted for the pressure variability recorded by the bottom pressure record we would expect that it might be larger in years with longer mooring configurations. Therefore we conclude that the pressure records from the deep moorings are primarily representative of changes in SSH.

To examine the impact of the local winds on the hydrographic variability we use the European Center for Medium-Range Weather Forecasts (ECMWF) ERA-Interim reanalysis [*Berrisford et al*., 2009]. This is a global forecast model that is forced by observations to produce a consistent best approximation of the state of the atmosphere every 6 h on a horizontal grid of 80 km resolution. The product has been shown in previous studies to represent the magnitude, size and location of wind jets along the southeast coast of Greenland satisfactorily [*Harden et al*., 2011]. For this study, we utilize the 10 m wind field and mean sea level pressure fields on 6 hourly time steps.

For much of the analysis we use the model derived surface stress. However, there is no guarantee that this surface stress equates to momentum input into the ocean because we have seasonal and mobile sea ice along

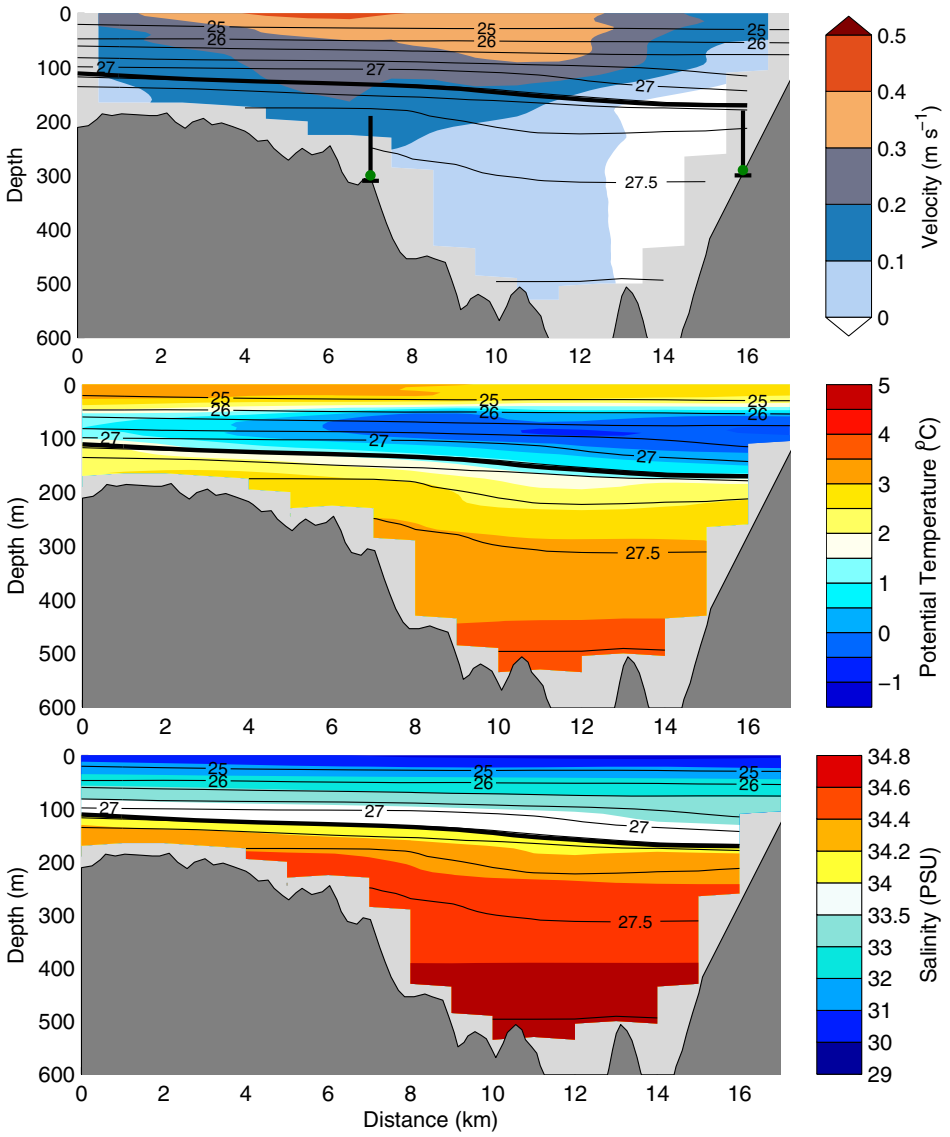

Figure 2. Mean over the 5 years of repeat sections. The Greenland coast is to the right of the section. (top) Mean absolute geostrophic velocity (m s^{-1}) referenced to detided LADCP data. Positive velocities are equatorward through the section. Potential density contours (kg m^{-3}) are overlayed. The solid black line is the 34 psu isohaline and marks a boundary between the Polar and Atlantic layers. The green markers indicate the approximate positions and depths of the (left) OFF and (right) ON moorings and the black vertical lines shown the approximate depth range covered by the thermistor strings. (middle) Mean potential temperature (°C) with potential density and 34 psu isohaline overlayed. (bottom) Mean salinity (psu) with potential density overlayed. See Figures 3–5 and Table 2 for more details on the individual sections.

the coast. Previous studies have shown that the input of momentum from the winds is not trivially related to the concentration of sea ice [*Williams et al.*, 2006; *Schulze and Pickart*, 2012; *Oltmanns et al.*, 2014]. ERA-Interim uses a relatively course ice model and *Outten et al.* [2009] show momentum transfer along the Marginal Ice Zone is generally problematic in this region. However, until these issues can be resolved, the model surface stress is the best option for assessing the potential momentum input to the ocean from the atmosphere.

3. Synoptic Sections

The mean of the five synoptic crossings shows a similar picture to that seen in previous realizations of the East Greenland Coastal Current [*Bacon et al.*, 2002; *Wilkinson and Bacon*, 2005; *Sutherland and Pickart*, 2008]. A wedge of buoyant, fresh water sits above and onshore of denser, saltier water (Figure 2). Salinity dominates the density signature and the horizontal density gradient supports a surface-intensified velocity signature mostly contained within the top 200 m of the water column. This mean is robust; each of the five crossings exhibits the same current structure. (Figures 3–5).

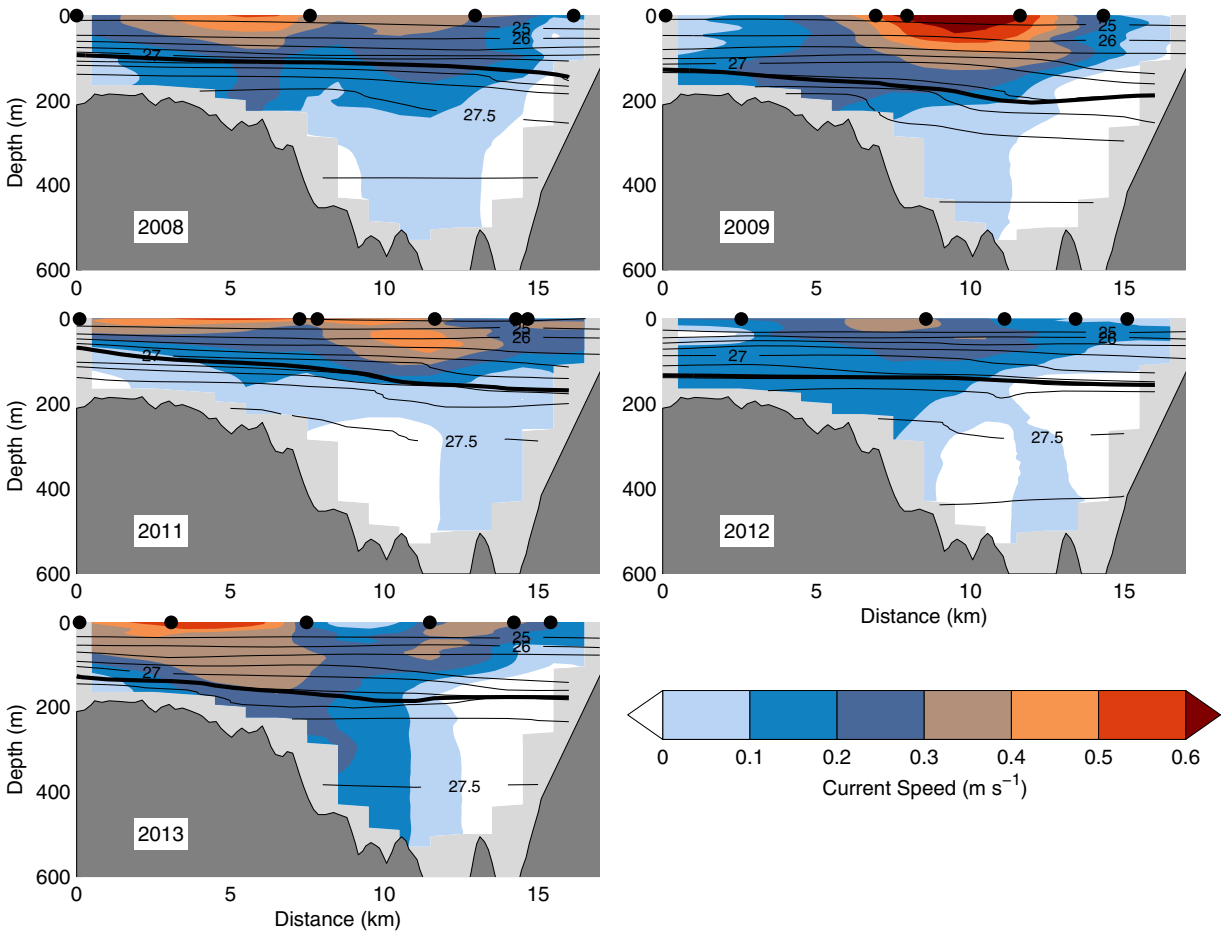

Figure 3. The five sections of absolute geostrophic velocities with potential density contours overlayed (kg m^{-3}). 34 psu isohaline shown with thick black line. Black circles indicate the locations of the CTD profiles used in generating the sections. See Table 2 for more details on the individual sections.

In all sections, the hydrographic characteristics below approximately 100 m (salinities greater than 33 psu) show two water masses with Θ-S properties lying on a mixing line between them (Figure 6). At the bottom we see Atlantic Water, which has encroached onto the shelf from the Irminger Sea, and above this we see Polar Water that originated in the Arctic and has been transported southward in the East Greenland Current probably with some modification en route. Near the surface, the Polar Water has been modified by seasonal surface heating to form a warm, but fresh layer.

The Atlantic and Polar layers are mixed at their interface so a robust definition of the depth of this interface is not trivial. The Θ-S properties (Figure 6) show that the 34 psu isohaline reasonably demarcates the water masses and so we will use this as the definition of the interface throughout the paper.

The mean velocity signature in the sections shows that the bulk of the East Greenland Coastal Current is mostly confined to the width of the channel (∼15 km). This is seen also in each individual section and corroborates previous studies that have suggested that the current is narrowing and forced closer to shore through this region [*Bacon et al.*, 2002; *Sutherland et al.*, 2013].

The mean volume transport through the section over the 5 years is 0.66 ± 0.18 Sv with a range from 0.44 ± 0.17 Sv in 2012 to 0.84 ± 0.16 Sv in 2013. The mean freshwater transport through the sections is 42 ± 12 mSv with a range from 26 ± 6 mSv in 2012 to 55 ± 7 mSv in 2013 (Table 2).

Both the total and freshwater transports fall nearer the lower end of their respective historic ranges (Total: 0.2–2.0 Sv, Freshwater: 10–100 mSv) [*Bacon et al.*, 2002; *Wilkinson and Bacon*, 2005; *Sutherland and Pickart*, 2008]. Given that we also find velocity maxima on the edge of our sections, it is probable that we are

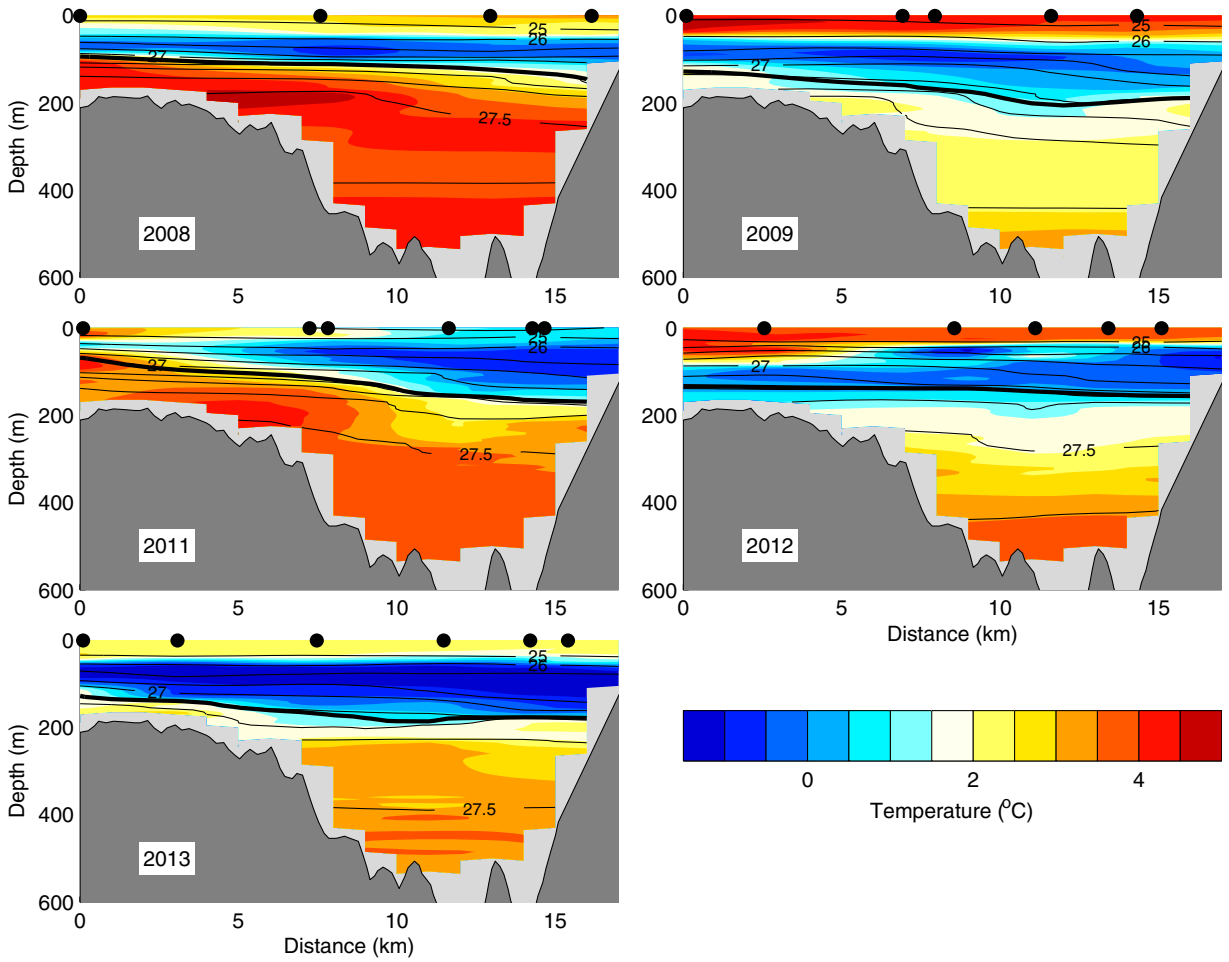

Figure 4. As Figure 3 but for the five sections of potential temperature (°C).

missing a portion of the current from our transport estimates in some years. Our values are therefore probably an underestimate of the complete transport in the current.

The relative abundance of the two water masses varies between years (see Table 2). The depth of the interface between the Polar and Atlantic Waters (34 psu isohaline) is at 142 m in the mean but has a range of 54 m about this value. There is no correspondence between the depth of the 34 psu isohaline and the transports measured. However, there is very good correlation between the mean depth of the 33 psu isohaline and both the total ($r = 0.94$) and freshwater transports ($r = 0.79$), corroborating the findings of *Wilkinson and Bacon* [2005]. However, in our case, we only have five points for our correlation and we would need more sections to increase the robustness of this result. The lack of correlation deeper in the water column could be due to the larger influence of stratification changes in the Atlantic water layer as can be seen in Figure 6.

As a final note, the five-section means are our estimate of the mean summertime transport through this section. However, the individual section transport estimates should not be seen as necessarily representative of interannual variability. We will show that the depth of the Polar layer in the current undergoes significant synoptic variability. The transport measurements from the sections may not be representative of the years in question; they are simply isolated snapshots of a variable current in the summertime.

4. Moored Hydrography

The full time series from the fixed CTDs and the thermistors are shown in Figures 7 and 8, respectively. The summertime sections discussed above give us the context through which we can interpret this data.

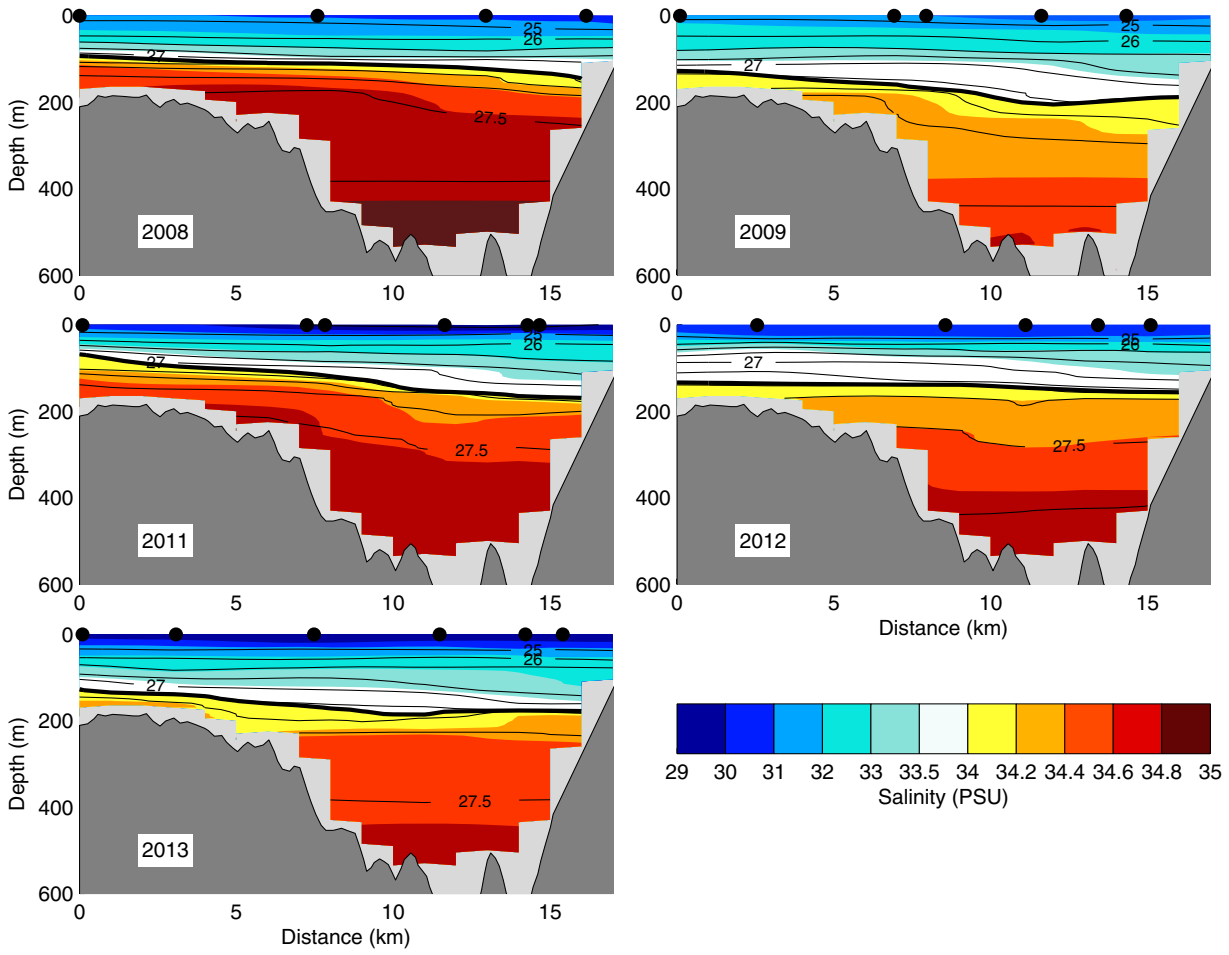

Figure 5. As Figure 3 but for the five sections of salinity (psu).

The first thing to note from the sections is that, at least in the summertime, the larger part of the flow in the East Greenland Coastal Current is confined to the 15 km wide channel where our moorings were placed. In addition, previous studies have shown that the current is narrowed and confined to the coast through this region through drifters [*Bacon et al*., 2002], instrumented seal dives [*Sutherland et al*., 2013], SST measurements [*Sutherland et al*., 2013] and model results [*Bacon et al*., 2014]. Our moorings are therefore capturing variability from a location within the East Greenland Coastal Current.

Second, the depth of the moorings are in the vicinity of the interface between the Polar and Atlantic Water (Figure 2). We clearly see both Atlantic and Polar water masses in the Θ-S properties from the moorings (Figure 9) with the majority of the water sampled lying on a mixing line between these two end-members. Although our moorings are too deep to truly capture this interface in the summertime, they are well placed to investigate its evolution throughout the rest of the year when the interface is deeper.

The limitations of our moored data are that we lack velocity data from the core of the current and so cannot assess the year-round transport. We also do not know how the current evolves laterally through the year, nor do we have data in the top 100–200 m. Unfortunately, given the current data availability we cannot resolve these limitations in the current paper. Having said that, an important factor for flow along the coast is the thickness of the Polar layer in the current; this plays a key role in the freshwater content and transport [*Wilkinson and Bacon*, 2005], the dynamics [*Sutherland and Pickart*, 2008] and how the current might force circulation in Sermilik fjord [*Straneo and Heimbach*, 2013]. As we will show, our moorings are well placed to investigate the evolution of the Polar layer depth for the larger part of the year in a region where the current is prevalent. As such, the lateral and vertical limitations of our data will not inhibit advancement of knowledge in this area.

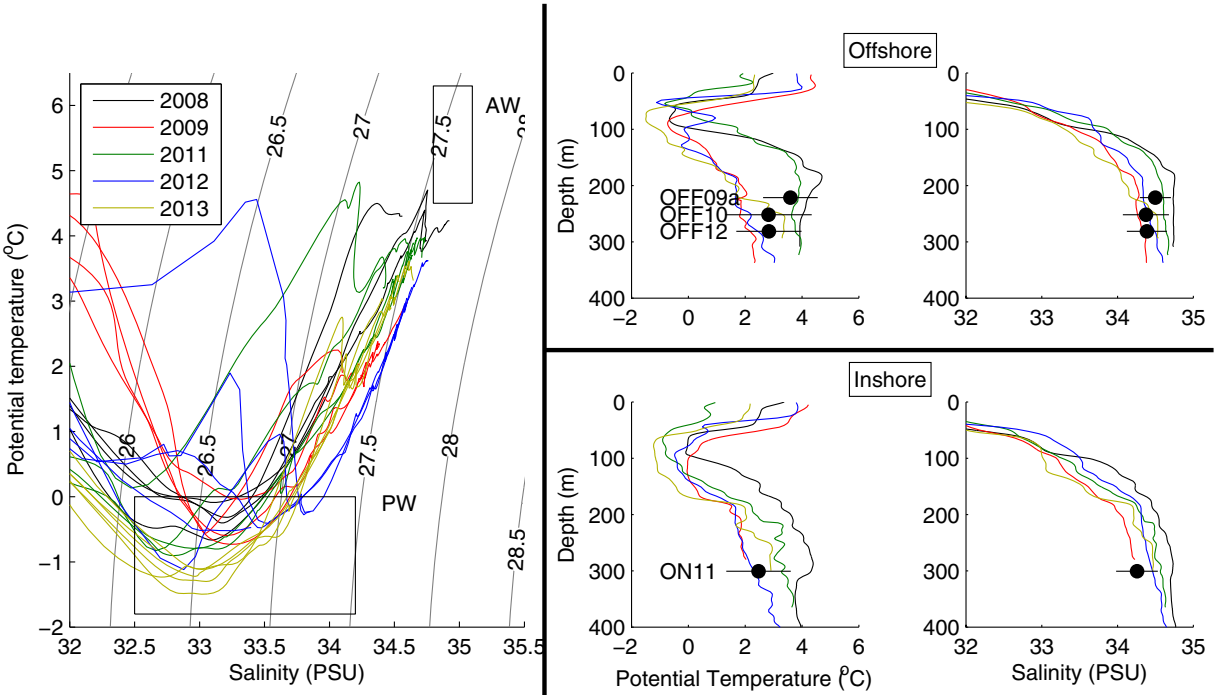

Figure 6. (left) The Θ-S properties of all profiles, colorcoded by year, that go into the five synoptic sections. The black boxes indicate typical end member regions for Polar Water (PW) and Atlantic Water (AW), an approximation of *Rudels et al.* [2002]. (right) Four plots showing the profiles of (left) potential temperature and (right) salinity for the nearest CTD profiles to the moorings on the (top) offshore and (bottom) onshore side of the channel. Colors are as in θ-S plot. The depth and property means from the moorings are shown by black dots with the black bar ranging ± 1 standard deviation.

4.1. Seasonal Characteristics

We begin our analysis of the moored data by examining the seasonal changes. As noted, the hydrographic properties measured over each year primarily lie on a mixing line between Polar and Atlantic Water end members (Figure 9). There is some seasonal variability in this though, both in the specific properties of each of the two end members and in the robustness of the mixing line. To see these seasonal changes clearly, we made a linear fit to the Θ-S data at each time step using a 30 day window around that time. We determined the quality of the fit at each time by the correlation coefficient of the scatter (Figure 10).

For the most part the hydrographic properties measured by the fixed-depth CTDs follow a tight, linear mixing line between Polar and Atlantic end members (Figure 10—very high correlation) but in every year, the mixing line becomes less pronounced in the fall months (reduced correlation) and is less clearly defined as a simple mix of waters from Atlantic and Polar origins. In the fall, temperatures tend to be higher (Figure 7) and sporadic warm water intrusions are clearly visible at the top of the thermistor record especially in the

Table 2. Section Statistics[a]

Year	Interface Depth (m) (34 psu Isohaline)	Density (kg m^{-3}) 100 m	Density (kg m^{-3}) 250 m	Transport (Sv)	FW (mSv)
2008	114	26.98	27.54	0.70 ± 0.19	38 ± 5
2009	168	26.76	27.36	0.70 ± 0.17	43 ± 6
2011	124	26.97	27.48	0.63 ± 0.16	46 ± 5
2012	142	27.03	27.49	0.44 ± 0.17	26 ± 6
2013	163	26.72	27.46	0.84 ± 0.16	54 ± 7
Mean ± 1 SE	142 ± 24	26.89 ± 0.17	27.47 ± 0.08	0.66 ± 0.18	42 ± 12

[a]Statistics from the five synoptic sections taken over the width of the East Greenland Coastal Current and shown in Figures 3–5. Values shown are the mean depth of the 34 psu interface, the density at 100 m and 250 m, and the total volume and freshwater (FW) transports. Errors quoted for individual transport estimates are a combination of geopotential height errors across the section and uncertainties in tidal and other ageostrophic flows—see *Sutherland* [2008, Appendix 1] for full details. The bottom row indicates a standard error (1 SE). This is calculated using the standard formula for estimating a population mean from a number of independent samples.

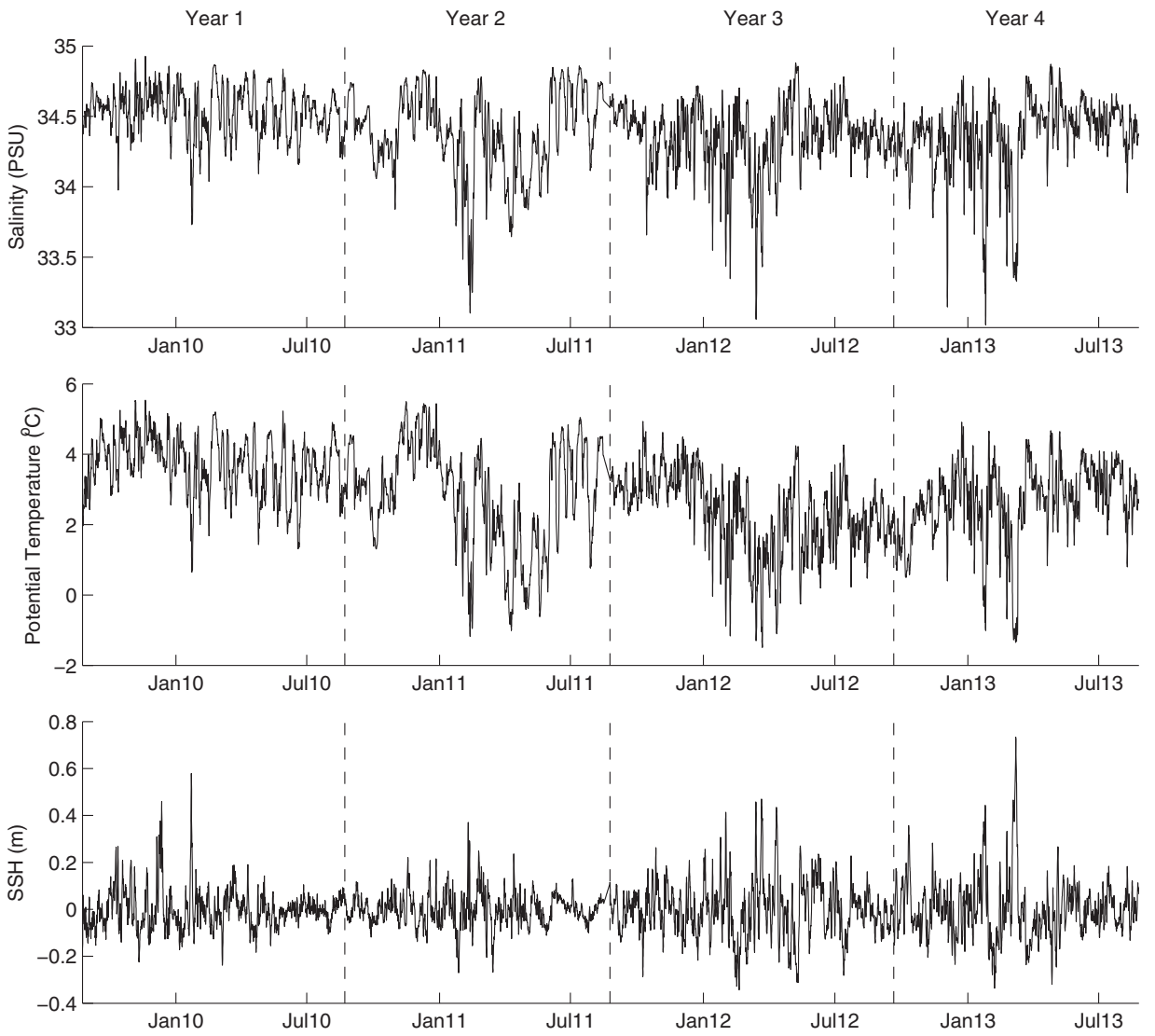

Figure 7. The complete combined time series from moorings OFF09 (year 1), OFF10 (year 2) and ON11 (years 3 and 4) showing (from top): Salinity, Potential Temperature and Sea Surface Height (SSH). Vertical dashed lines delineat the deployment years. NB: The record for year 4 comes from the ON11, not from the concurrent mooring OFF12.

records from OFF09a and OFF10 when the moorings were on the offshore side of the channel (Figure 8). A breakdown of the typical paradigm of Polar Water over Atlantic Water occurs at these times.

These features are reminiscent of warm water intrusions tracked from the shelf break up to the mouth of Sermilik fjord through instrumented seal dives by *Sutherland et al*. [2013]. They were able to show a seasonality in the prevalence of full-depth warm water profiles, which peaked in the fall period. Our results support their evidence that during the fall Atlantic Water is able to penetrate toward the coast at shallow depths, possibly as full-depth Atlantic Water profiles. This forces the Polar Water of the East Greenland Coastal Current to be moved inshore and shoaled. This also supports our claim that the current is confined to the channel at the time of the year when the synoptic sections were taken.

For the rest of the year we have a more typical two layer system and tight linear fits to the Θ-S properties exist. The gradient and intercept of this line varies throughout the year and between years though, indicating seasonal and interannual modification of the end members. The mean seasonal mixing lines for all years are shown in Figure 10. Although there are interannual offsets, the seasonal pattern is robust in all years. The Polar Water becomes denser from winter through to summer most likely due to progressive winter and

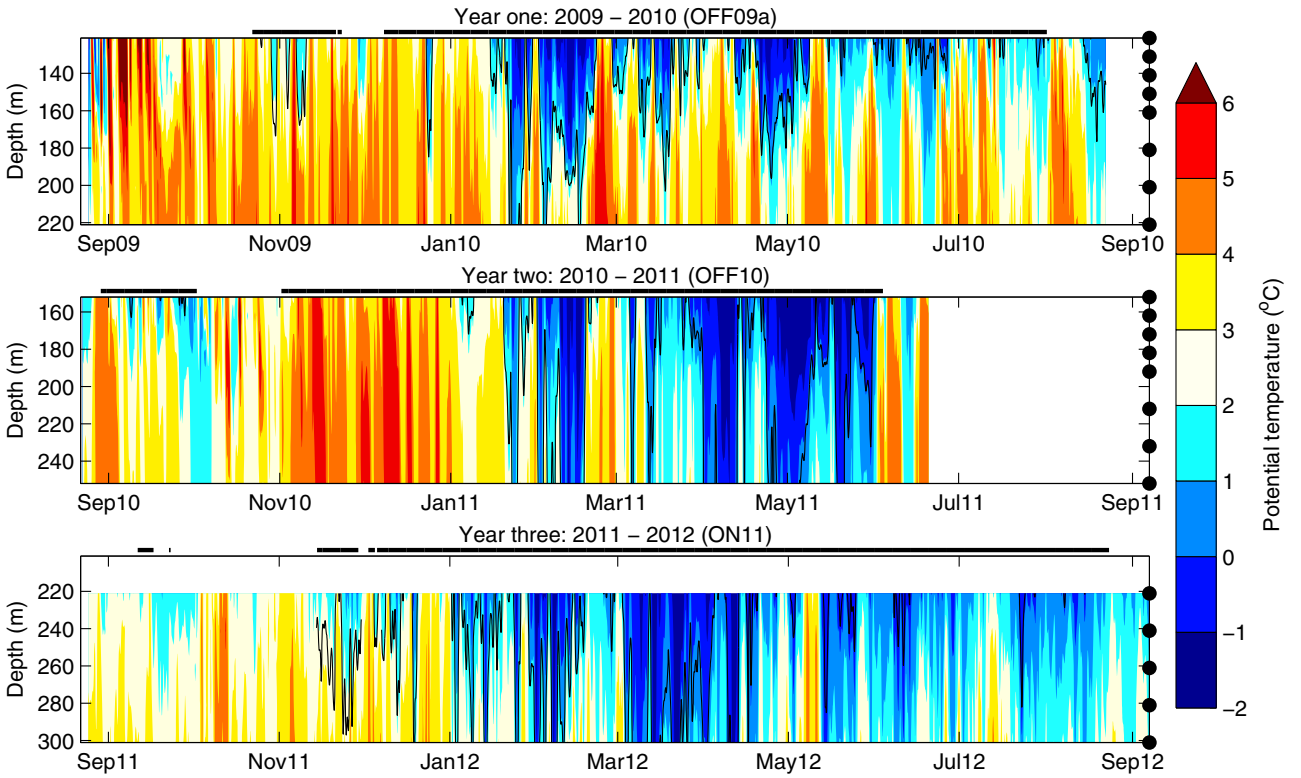

Figure 8. Temperature record from the 3 years of thermistor chain deployment (year 1: OFF09a, year 2: OFF10, and year 3: ON11). Absolute depths vary between record, but the depth range is constant. Instrument depths are shown on the right axis with black dots. Plotted in black is the 34 psu isohaline as calculated from the time-varying Θ-S properties shown in Figure 9, which acts as a guide to the interface between Polar and Atlantic water masses. The salinity field was calculated for all times when there was a good linear fit for the TS properties ($r > 0.9$, see Figures 9 and 10). The times when salinity was calculated are shown with a solid black bar on top of each record.

spring modification from winds and sea ice formation en route down the Greenland coast. The Atlantic Water is warmest in the summer (and fall, when we have the full depth intrusions, but no consistent linear Θ-S relationship) and coolest in the spring demonstrating that seasonal signals in the Atlantic Water, presumably generated when the water was nearer the surface in the Irminger sea, are maintained as the water penetrates onto the shelf. This suggests a short advective timescale.

The seasonally varying mixing lines indicate that the temperature records from the thermistors do not constitute a time-invariant proxy for salinity or density. Taking account of the seasonal and interannual variability in the mixing lines allows us to convert the thermistor record to salinity and density over the periods when there was a robust mixing line (non-fall months, $r > 0.9$). We additionally define a mean stratification at each time by the difference in density over the depth of the thermister record.

The relative abundance of Polar and Atlantic Water in the current changes seasonally—of particular note is the seasonal swelling of the freshwater content in the current. Between mid-winter and early summer each year the thermistor record clearly shows more frequent and deeper Polar Water occurrences that are colder than 0°C and fresher than 34 psu (Figure 8). During these times, the density at the fixed-depth CTDs is also lower on average by 0.2 kg m^{-3} and this is concurrent with an increase in stratification over the depth of the thermistor chain (Figure 11). Our interpretation is that from mid-winter into spring and early summer, the Polar layer thickens and the halocline is brought down over the moorings, which allows the thermistors to see the steeper density gradients in the Polar layer (e.g., Figure 6).

The limitations of our data are such that we do not know over what lateral range this seasonal signal is spread. However, two previous studies [*Straneo et al.*, 2010; *Bacon et al.*, 2014] note a shelf-wide deepening of the Polar layer in phase with ours indicating that our seasonal signal is not just confined to our study area, but is representative of the wider East Greenland Coastal Current. We will discuss potential causes of this seasonality in Section 7.

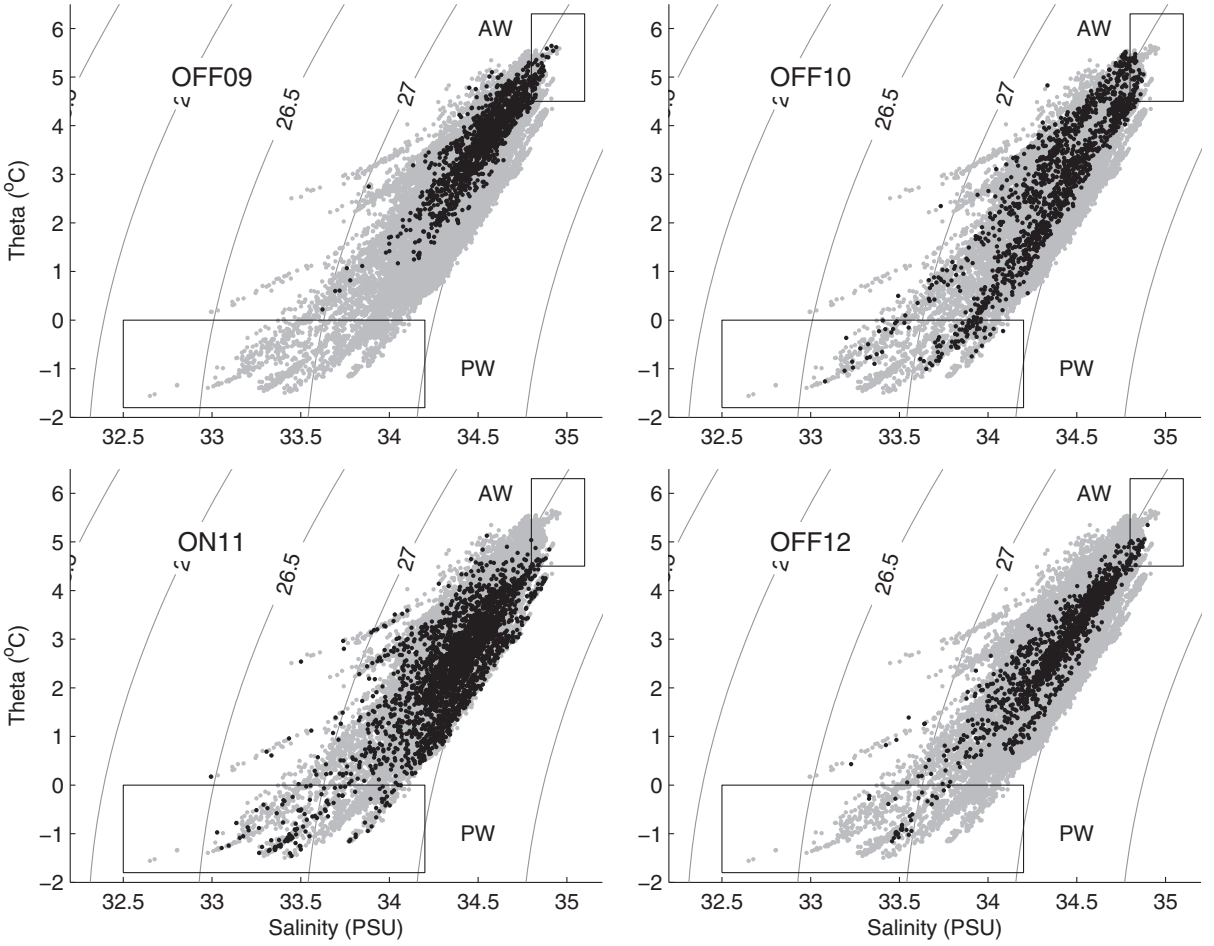

Figure 9. Θ-S scatter diagrams for the four moorings deployed over the 4 years. In each plot, the grey scatter is the Θ-S from all four moorings and the black scatter are for the particular mooring in question. Black end member boxes are as Figure 6.

4.2. Synoptic Variability

The fact that we can observe robust submonthly mixing lines over much of the year demonstrates that a major signal in the data is variability along this mixing line at shorter than monthly time scales. In fact, significant variability on scales as long as monthly and as short as daily are clearly discernible in all years (Figure 7).

This variability is expressed as large vertical excursions of isotherms (Figure 8) often larger than the depth range of the record (∼100 m). It is clear, especially in the non-fall months, that the submonthly variability measured by the fixed CTDs represent significant changes in the relative quantities of Polar and Atlantic Waters in the current as the interface between the layers over our moorings is raised on lowered.

The submonthly variability occurs in concert across the width of the channel (∼10 km). For years 3 and 4, the mooring location was moved from the offshore side of the channel to the onshore side. In association with this move is an increase in the magnitude of the variability in the 1–2 day period (visible in Figure 7). However, in year 4 when we also have synchronous measurements from either side of the trough, the records covary much more significantly than they demonstrate cross channel variability (not shown). Our conclusion is that most of the variability discussed above is expressed in concert over the width of the channel. However, it should be noted that we do not know how representative the synoptic scale variability is of the wider shelf in this region. This is especially important in the winter and spring when we have no evidence that the East Greenland Coastal Current is necessarily confined to our study region. Unfortunately this limitation is beyond the currently available data.

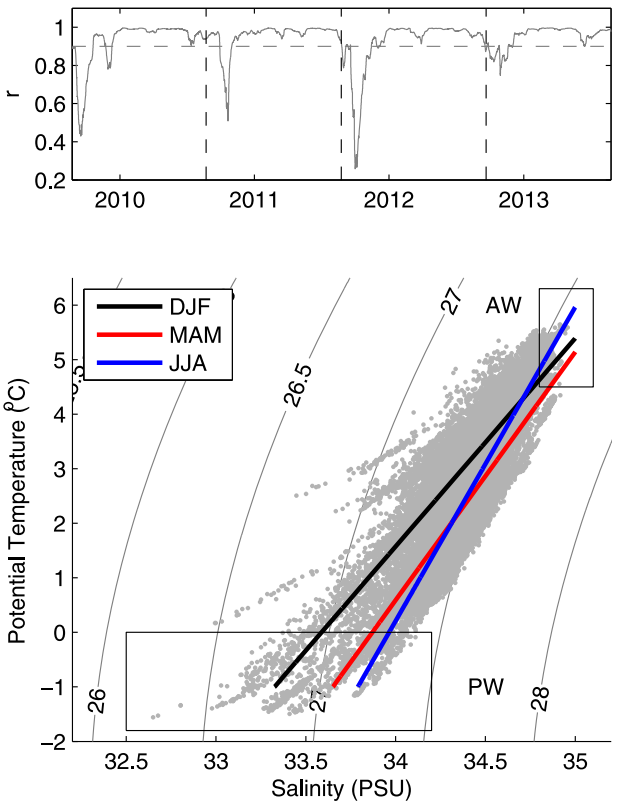

Figure 10. The seasonal evolution of the Θ-S properties. (top) Correlation coefficient of linear fit to Θ-S properties (see Figure 9) over a 30 day window. (bottom) Scatter of all points in Θ-S space from all four moorings (gray). Overlayed are the mean linear fit lines for three seasonal periods. Black end member boxes as Figure 6.

There are seasonal patterns to the synoptic variability that shed light on the possible drivers (Figure 11). The variability on submonthly scales is enhanced through the winter and spring months in all years (Figure 11, more so in years 2–4). Two factors that might be forcing this seasonality are a deeper halocline and the action of winds.

Firstly, as previously discussed, the density measured at the fixed CTDs decreases during the winter and spring while the mean stratification increases due to a thickening Polar layer (Figure 11). The implication for the submonthly variability is that any displacement of isopycnals at these times would produce larger changes in density than in the summer when the stratification at the depth of the moorings is weaker. Between summer and spring the average stratification changes from 0.1 to 0.3 kg m^{-3}(100 m)$^{-1}$ whilst the mean standard deviation of the density changes from 0.05 to 0.15 kg m^{-3}. The vertical heaving needed to produce the density changes at the fixed CTDs is therefore 50 m regardless of the season. This is a typical vertical displacement of isotherms we observe in the thermistor record (Figure 8) suggesting that a deeper halocline is a major cause of the increase in the density variability during the winter and spring.

The second factor that could be influencing the larger variability in the winter months is the concurrent enhancement in the strength and frequency of the along-coast winds. This also occurs in concert with both enhanced density variability (Figure 11) and SSH variability (Figure 7). We will argue in Section 5 that coastal winds can force downwelling and are an important driver of density changes at the coast. Regardless of the specific response of the shelf to the winds though, the fact that there is a ready source of energy at the surface that covaries with the seasonal variability seen in the hydrography gives weight to the influence of winds in some manner.

5. Wind Forcing

In this section we focus on wind forcing of the hydrographic changes in the East Greenland Coastal Current. It is probable that the buoyancy-driven current might also be intrinsically unstable to baroclinic disturbances, i.e., the horizontal density gradient could become large enough to drive instabilities in the front and produce oscillations or eddy shedding. However, due to the limited spatial extent of our moored data we do not address this here.

We instead focus on the downwelling impact of along-coast barrier winds. Barrier winds are strong, low-level winds that frequently occur along the southeast coast of Greenland [*Moore and Renfrew*, 2005; *Harden et al*., 2011]. They form when stable air is forced toward the high coastal barrier. Unable to climb the steep topography, the air is channeled coast-parallel into an intense wind jet. The atmospheric configuration

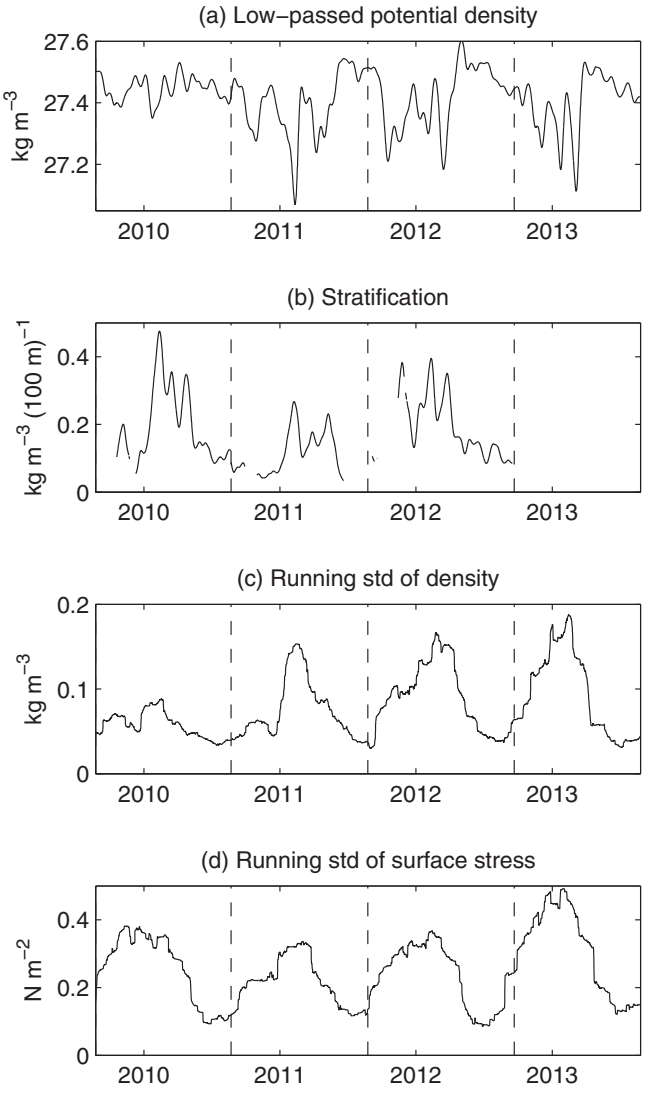

Figure 11. Seasonal evolution of the hydrography and wind field. (a) Potential density from fixed CTDs low-passed at 30 days using a Butterworth filter. (b) The stratification over 100 m low-passed over a 30 day window. (c) The running standard deviation over a 30 day window of the potential density, low-passed at 30 days. (d) The 30 day moving window standard deviation of the 30 day high-passed along-coast surface stress (measured relative to 45° from north) from ERA-Interim at a location just offshore of Sermilik Fjord (see Figure 12 for location and complete time series).

typical of barrier winds is shown in Figure 12. Winds in excess of 20 m s^{-1} are a weekly occurrence in wintertime [*Harden et al*., 2011] although strong winds of these type can occur throughout the year (Figure 12). Sermilik Fjord also happens to be at a location of local wind enhancement [*Harden and Renfrew*, 2012] ensuring some of the strongest along-coast wind events occur in the region of the moorings. *Sutherland and Pickart* [2008] showed that barrier winds can steepen the front of the East Greenland Coastal Current and drive an increase in along-coast transport. Evidence of downwelling and shelf wave formation forced by barrier winds has also been observed as far out as the shelf break [*Harden et al*., 2014].

5.1. Impact of Barrier Winds

We have shown that the energy of the wind field covaries with the energy in the hydrographic signal on seasonal time scales. We will now attempt to explain the exact impact of the winds on the sub-monthly variability.

Given the relative spatial paucity of our data and the fact that we lack velocity measurements, we will focus on the effect of downwelling. In theory, when a barrier wind blows, a surface Ekman layer will be set up that will transport water onshore [*Lentz and Largier*, 2006]. This water would build up and generate a sea surface height (SSH) gradient perpendicular to the coast. This gradient would not only force an along-coast geostrophic acceleration, but will drive downwelling near the coast and an offshore flow below the surface layer. From the perspective of our moorings near the coast, this would look like a reduction in density during a build up of SSH.

The along-coast wind velocity (relative to 45° from north) correlates significantly with the density record (from the time series shown in Figure 7) at a maximum of $r = -0.50$ in a broad region along the southeast coast of Greenland (Figure 13). The sign of the correlation is negative, which indicates a reduction in density during an increase in equatorward wind speed, consistent with downwelling. The extension of this region upstream and downstream of the mooring site is probably reflective of the good coherence of the wind velocities along the coast. The correlation maximum though, is near colocated with the mooring indicating the need for local forcing to produce the downwelling signal.

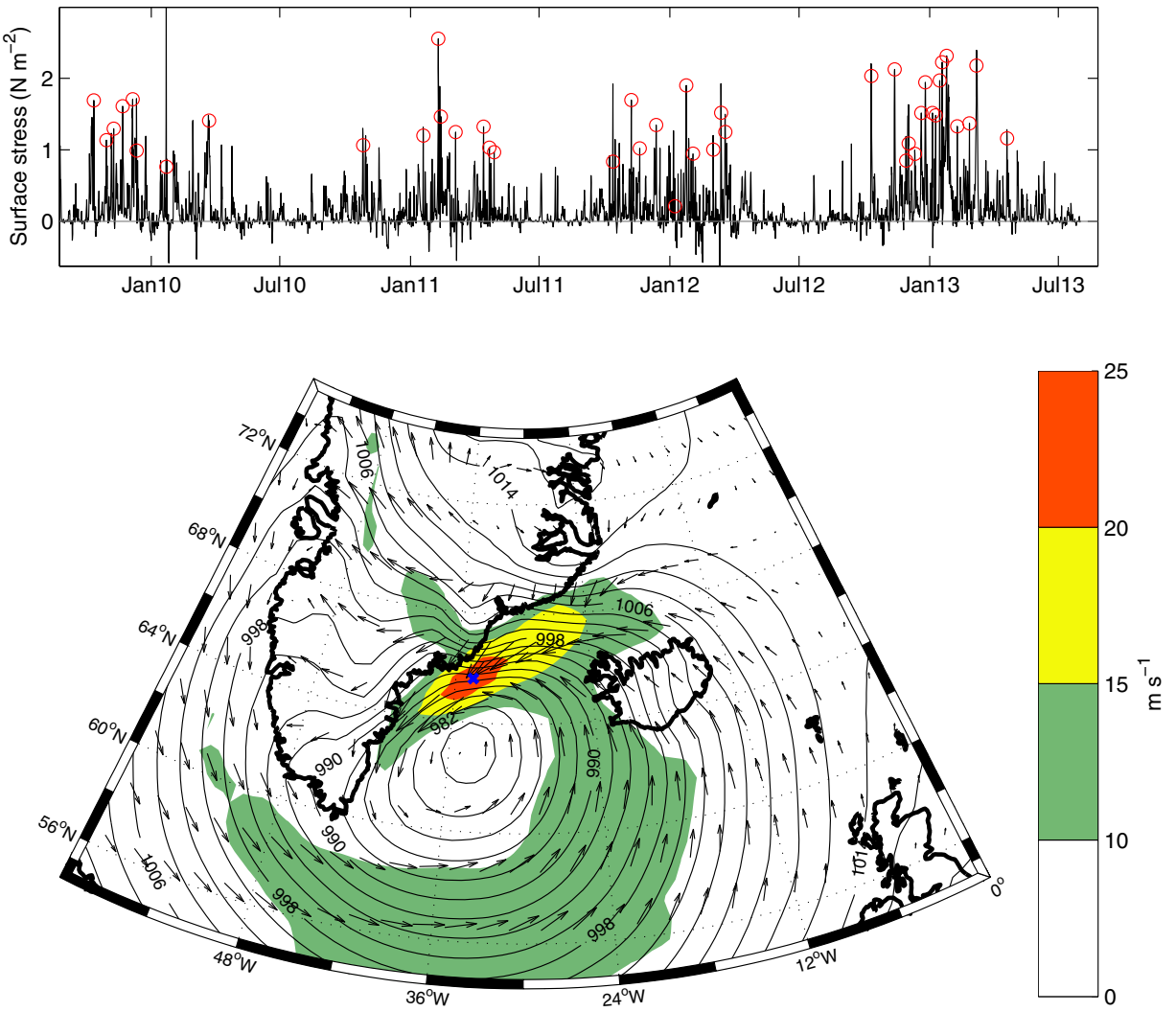

Figure 12. (top) Along coast surface stress (N m^{-2}, measured relative to 45° from north) over the period of the mooring deployments from the location shown with a blue cross in the bottom plot. (bottom) Composite image of the 10 m wind field and mean sea level pressure for the times of wind events over 15 m s^{-1} shown by red circles in top plot.

This density correlation signal is enhanced if the analysis is conducted only using the density record from ON11 (the mooring on the onshore side of the trough). The most significant change we observed when moving from the offshore side to the onshore side of the trough was an increase in energy on periods of 1–2 days. It could be that the onshore side of the trough is more sensitive to wind forcing on these scales.

The along-coast wind velocity also correlates well with the SSH measured at the moorings (Figure 13). The positive correlation is the signature of a build up of coastal SSH when the wind blows. The pattern is slightly different to the density signal in that the broad region of good correlation (peaking at $r = 0.50$) is centered upstream of the mooring site and slightly further offshore. This probably reflects the potential for barrier winds to excite coastally trapped waves that will propagate downstream toward the mooring site from any upstream center of action [*Harden et al.*, 2014].

The density and the pressure records are anticorrelated in the ON11 record from the onshore side of the channel (Figure 7); an increase in SSH is associated with a decrease in density consistent with the signature of downwelling. This anticorrelation between SSH and density is less pronounced on the offshore side of the channel again suggesting that the onshore side of the channel responds more readily to wind forcing.

To analyze individual downwelling-like events, we developed a detection routine. We have shown that the density variability is enhanced during the winter periods, in part due to the lowering of the

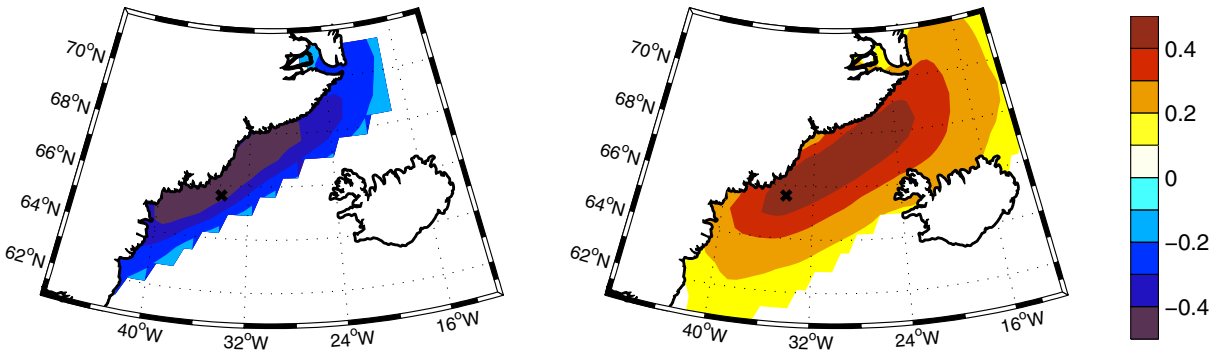

Figure 13. Maximum of the lagged correlation between the along coast wind (measured relative to 45° from north) at all points in the domain with (left) the potential density and (right) the pressure anomaly measured by the moorings for all 4 years of mooring deployments. The black cross shows the location of the time series used as a proxy for the wind field at the mouth of Sermilik Fjord in Figures 12 and 14. Only correlation values that are significant at >95% confidence are shown.

pycnocline. In order to not bias our analysis of the ocean in favor of these months, our detection routine takes this seasonality into account. We defined a low density event (one that may be consistent with downwelling) as a minimum in the density time series that is lower than two times the 30 day running standard deviation. i.e., a time when the density is anomalously low compared to the 30 days around it. The total number of events found in each mooring record is shown in Figure 14. The record from ON11 (from the onshore side of the channel) exhibited a proportionally higher number of events.

Lagged composites of the density response during these events show that the density remains anomalously low for a period of 2 days (Figure 14). At the same time as this drop in density comes an increase in SSH (for all records other than OFF10) and an along coast wind event 24 h before. This is again consistent with the impact of downwelling favorable winds; when the wind blows, there is an increase in SSH and a lowering of isopycnals.

This is not to say all wind events produce downwelling—on average, 64% of downwelling-like events were concurrent or preceded by less than 36 h by a wind event greater that 10 m s^{-1}. A similar analysis was conducted by examining the ocean response to the wind events highlighted in Figure 12 (not shown). The same pattern of a statistically significant increase in SSH and a lowering of isopycnals was found in the mean, but again, not all wind events triggered a downwelling-like response. In fact, for the records from OFF09 and OFF10, only 35% of wind events produced the desired effect, jumping to 55% for the ON11 record.

Our results show the expected response of downwelling and demonstrate that winds drive a significant proportion of the hydrographic variability in the East Greenland Coastal Current. However, it is also clear from the analysis that winds are not the sole driver of variability. There are clearly hydrographic changes that occur in the absence of winds. OFF10, for example, measures significant variability, but an insignificant response due to wind-forced downwelling (although the form of the SSH response is mirrored in the composite wind profile giving weight to our interpretation that winds are at least driving SSH changes). *Bacon et al*. [2014] argue for an equal importance of wind and buoyancy forcing to measured seasonal transports; it may be that the action of both is influential in driving dynamics on synoptic scales also.

6. Summary

Our study has focused on the hydrographic variability in the East Greenland Coastal Current in the Ammassalik region, southeast Greenland. In this region, a narrow channel (∼15 km wide) funnels the current past the mouth of the Sermilik fjord.

The mean synoptic sections of flow through the channel show a configuration seen in previous realizations of the East Greenland Coastal Current. A wedge of cold, fresh Polar Water sits onshore and atop warm, salty Atlantic Water with the horizontal density gradient supporting a surface intensified current. In all sections, a significant quantity of the current flows through the channel arguing for a narrowing of the current in the region (at least in the summer time). There is variability in the total transports (0.66 ± 0.18 Sv), the freshwater transport (42 ± 12 mSv referenced to 34.8 psu), and in the thickness and arrangement of the Polar

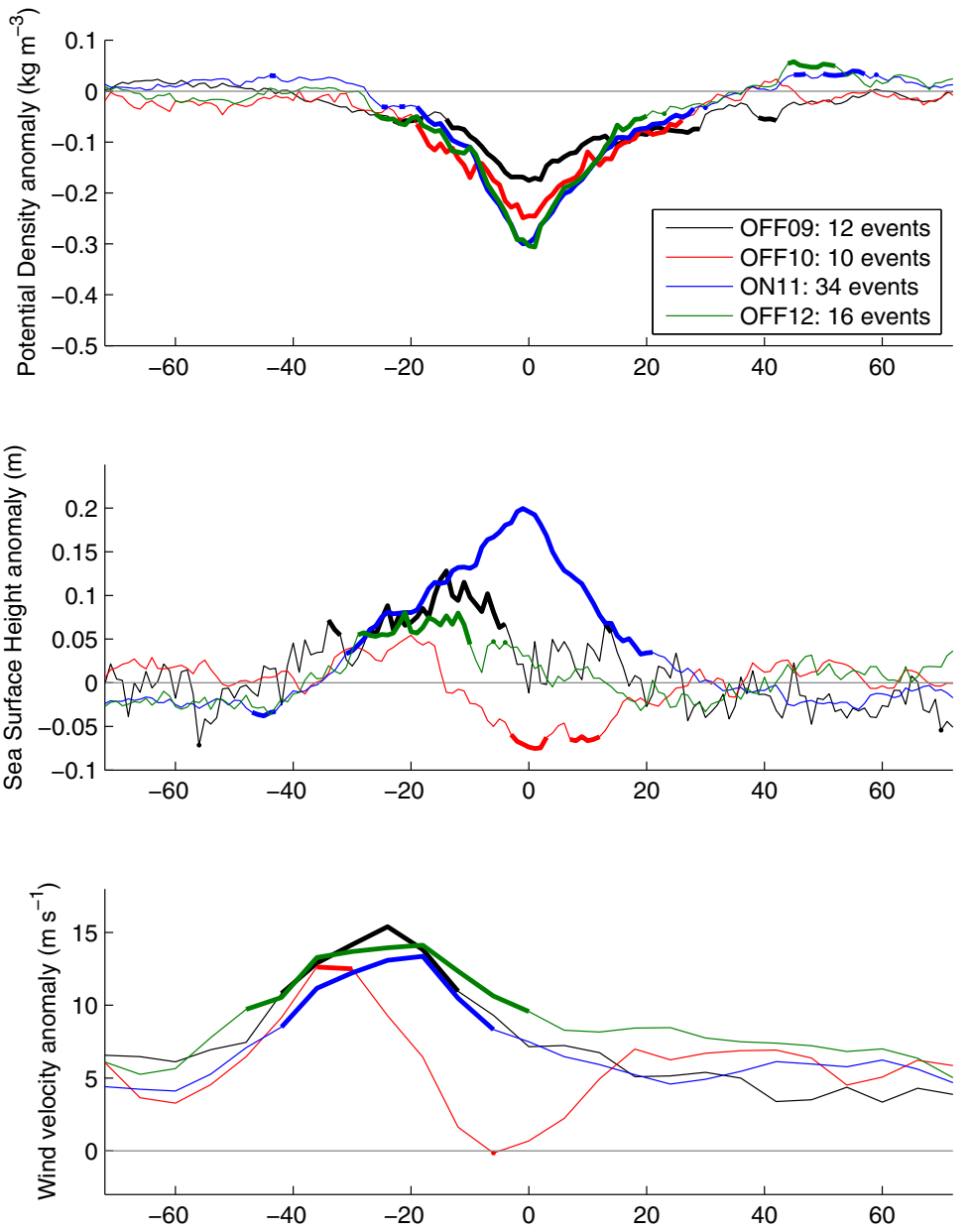

Figure 14. Lagged composites of (from the top) potential density (highpassed at 90 days), SSH anomaly and along coast wind velocity for the times of low density events measured at the mooring. Each composite is broken down by mooring record (colors). Thick lines are shown for composite values that are distinctly different from the background variability with a confidence of 95%.

layer. From these five sections it appears that a deeper Polar layer (as measured by the 33 psu isohaline) forces both increased total and freshwater transports. It should be noted though that in some sections we do not completely capture the full velocity signature of the current indicating that our transports are probably slight underestimates.

Our moored time series allowed us to explore year-round variability. Our main conclusion is that in this region, the current undergoes large variability on previously unresolved submonthly time scales. This is manifested as large vertical movements (at times larger than 100 m) of the isotherms over the width of the channel (∼10 km) on time scales as short as daily and as long as monthly. The magnitude of this variability increases throughout the winter, the result of one or both of a seasonally lowered pycnocline and more variability forced by the winds.

On seasonal scales, our data corroborates previous studies that have shown that in the fall period, the East Greenland Coastal Current at our location is hemmed in toward the shore by the increased presence of shallow Atlantic Water that has flowed in from the shelf break. In other seasons, a more robust two layer system is seen near to the coast with Polar Water overlaying Atlantic Water. The Polar Water deepens throughout the winter and into the spring increasing the freshwater content of the current. In Section 7 we will argue that this is primarily due to the seasonality in the export of freshwater from the Arctic.

A signal consistent with downwelling forced by along-shore barrier winds is observable at the moorings, although the response appears to be stronger nearer to the coast. This argues for a significant impact of the winds on the high-frequency variability in the coastal current. There is clearly variability not described simply by downwelling favorable winds though. It is likely that other wind-forced process and/or internal instabilities are driving variability in the current. Unfortunately, our data are insufficient to characterize these processes at present.

7. Discussion

7.1. Seasonal Evolution

Our data show that the Polar layer in the current deepens through the winter and spring. Other studies have shown that this is a shelf-wide phenomenon [*Straneo et al*., 2010; *Sutherland et al*., 2013; *Bacon et al*., 2014]. We will now discuss the possible drivers of the expanding freshwater content.

Locally, the along-coast wind field is stronger in the winter and spring (Figure 12). As discussed on synoptic scales, the winds force surface water toward the coast, downwelling the pycnocline and bringing more Polar water down to the depth of our mooring. This would probably result in a seasonal deepening of the Polar layer at the coast for periods of seasonally stronger winds. Although we cannot discount this as having a role in our mooring record, this mechanism alone would only result in a redistribution of a set volume of Polar water on the shelf into a thinner wedge near the coast. It can't account of the shelf-wide deepening of the Polar layer.

We are left requiring an external input of freshwater to account for the shelf-wide seasonality. One possibility is the seasonal melt water runoff from the Greenland ice sheet. This is unlikely to be a significant contributor though as the increasing freshwater content on the shelf is not in phase with the local inputs of freshwater from the Greenland ice sheet. The majority of export from the Greenland ice sheet occurs in the summer and fall [*Bamber et al*., 2012]. However, the swelling of the freshwater in the current from our measurements occurs between mid-winter and early summer.

Another source of freshwater is from sea ice melt along the coast. Most of this will occur after the sea ice maximum in February and March. Although this is a little late for the start of the increases in freshwater we show, we cannot discount it as having a role through the spring and into early summer.

Finally, the freshwater export (both as freshwater and ice) from the Arctic through Fram Strait undergoes a seasonality that could propagate down the coast of Greenland. The freshwater and sea ice fluxes through the Fram Strait are both largest in the fall and though the winter [*Kwok et al*., 2004; *de Steur et al*., 2009]. We therefore observe a lag of approximately 4 months between the freshwater content seasonality at Fram Strait and that measured at our moorings. Given a nominal distance of 1500 km, this equates to a mean advective velocity of $\sim$15 cm s^{-1} from the Fram Strait to our moorings. This compares reasonably well with previous measurements of velocities in the East Greenland Current [*Dickson et al*., 2008; *Hall et al*., 2011]. We therefore argue that the seasonal export of freshwater from Fram Strait is likely to be a significant driver of the winter deepening of the Polar layer in the East Greenland Coastal Current.

One implication of this result is that it supports the notion that the East Greenland Coastal Current is an inner branch of the wider East Greenland Current system, as proposed by *Sutherland et al*. [2009], and isn't primarily formed from runoff from Greenland as initially argued by *Bacon et al*. [2002]. Another implication is that a seasonally swollen current, coupled to possible increased barotropic acceleration from winds, might result in a larger freshwater transport during the winter than in the summer time. This corroborates the model results of *Bacon et al*. [2014] who show a doubling of total and freshwater fluxes between the summer and winter. As a community we may be low biasing our estimates of the freshwater flux in the East Greenland Coastal Current based mainly on summer time surveys; the current is probably far more important as a conduit for freshwater in non-summer months than we currently think.

7.2. Synoptic Evolution

Our moorings measured significant synoptic variability in the East Greenland Coastal Current at the coast. We have shown that synoptic changes occur in concert over our 10 km wide study area, but at present we cannot determine how the synoptic variability manifests itself over the wider shelf or how this will impact the current's freshwater content, velocity structure and dynamics. This is particularly important for the winter and spring months when we have no evidence that the Coastal Current is necessarily so confined to the coast as in the summer and fall.

As an example, the two drivers of synoptic changes we have discussed are likely to produce different forms of lateral variability. If winds were the primary driver of hydrographic changes in the current through downwelling then the freshwater content of the current would remain the same during a wind event, but would be redistributed to be a deeper, narrower wedge at the coast, presumably with a stronger current speed. However, if the hydrographic changes were being advected through the system (e.g., in the form of baroclinic instabilities) then the submonthly variability could be representative of absolute freshwater content changes with a different augmentation to the velocity field. At present we are unable to distinguish these processes and this highlights the importance of fully understanding the synoptic variability across the wider shelf in future studies.

East Greenland Coastal Current transports (from synoptic sections) have varied historically over an order of magnitude (0.2–2.0 Sv) both between years and spatially along the coast. The fact that we see such marked submonthly variability in the depth of the Polar layer and in the SSH (a proportion of which is wind-forced) might imply that the large range in historical transports is driven by synoptic variability. In light of this, we advocate for careful interpretation of any one synoptic section across the East Greenland Coastal Current. One section may not be thoroughly representative of the current at anything longer than synoptic scales.

In regards to the potential for the East Greenland Coastal Current to drive exchange between shelf and fjord waters, we have clearly demonstrated that large vertical excursions of isopycnals are possible on synoptic time scales. These appear to increase in magnitude though the winter and spring months. Furthermore, it appears that a combination of winds and internal variability are the drivers of these changes. Any analysis of fjord water mass variability must take into account the dynamics that would be the forced by this significant variability. Downwelling winds have already been cited as a driver of the exchange between the shelf and the fjord [*Straneo et al*., 2010], but our results highlight that there is more driving variability on the shelf than winds alone and other causes of variability should be considered.

Acknowledgments

The data used in this study will be made available at the National Oceanographic Data Center (www.nodc.noaa.gov). The processing and analysis code is available from the authors on request (bharden@whoi.edu). This work was funded by the National Science Foundation grant OCE-1130008, NASA grant NNX13AK88G, and the Ocean and Climate Change Institute at the Woods Hole Oceanographic Institution. Thanks to A. Ramsey and D. Torres for data processing. Thanks also go to the two anonymous reviewers for their comments that improved the quality and clarity of this paper.

References

Bacon, S., G. Reverdin, I. G. Rigor, and H. M. Snaith (2002), A freshwater jet on the east Greenland shelf, *J. Geophys. Res.*, *107*(C7), 3068, doi:10.1029/2001JC000935.

Bacon, S., A. Marshall, N. P. Holliday, Y. Aksenov, and S. R. Dye (2014), Seasonal variability of the East Greenland Coastal Current, *J. Geophys. Res. Oceans*, *119*, 3967–3987, doi:10.1002/2013JC009279.

Bamber, J., M. van den Broeke, J. Ettema, J. Lenaerts, and E. Rignot (2012), Recent large increases in freshwater fluxes from Greenland into the North Atlantic, *Geophys. Res. Lett.*, *39*, L19501, doi:10.1029/2012GL052552.

Berrisford, P., D. Dee, K. Fielding, M. Fuentes, P. Kallberg, S. Kobayashi, and S. Uppala (2009), The ERA-Interim Archive. ERA Report Series. 1. Tech. Rep. European Centre for Medium-Range Weather Forecasts, 16 pp., Shinfield Park, Reading, U. K.

Bersch, M., I. Yashayaev, and K. Koltermann (2007), Recent changes of the thermohaline circulation in the subpolar North Atlantic, *Ocean Dyn.*, *57*(3), 223–235, doi:10.1007/s10236-007-0104-7.

de Steur, L., E. Hansen, R. Gerdes, M. Karcher, E. Fahrbach, and J. Holfort (2009), Freshwater fluxes in the East Greenland Current: A decade of observations, *Geophys. Res. Lett.*, *36*, L23611, doi:10.1029/2009GL041278.

Dickson, R., J. Meincke, and P. Rhines (Eds.) (2008), *Arctic–Subarctic Ocean Fluxes: Defining the Role of the Northern Seas in Climate*, Springer, Dordrecht, Netherlands, doi:10.1007/978-1-4020-6774-7.

Hall, S., S. R. Dye, K. J. Heywood, and M. R. Wadley (2011), Wind forcing of salinity anomalies in the Denmark Strait overflow, *Ocean Sci.*, *7*(6), 821–834, doi:10.5194/os-7-821-2011.

Harden, B. E., and I. A. Renfrew (2012), On the spatial distribution of high winds off southeast Greenland, *Geophys. Res. Lett.*, *39*, L14806, doi:10.1029/2012GL052245.

Harden, B. E., I. A. Renfrew, and G. N. Petersen (2011), A climatology of wintertime barrier winds off southeast Greenland, *J. Clim.*, *24*(17), 4701–4717, doi:10.1175/2011JCLI4113.1.

Harden, B. E., R. S. Pickart, and I. A. Renfrew (2014), Offshore transport of dense water from the East Greenland shelf, *J. Phys. Oceanogr.*, *44*(1), 229–245, doi:10.1175/JPO-D-12-0218.1.

Holland, D. M., R. H. Thomas, B. de Young, M. H. Ribergaard, and B. Lyberth (2008), Acceleration of Jakobshavn Isbrae triggered by warm subsurface ocean waters, *Nat. Geosci.*, *1*(10), 659–664, doi:10.1038/ngeo316.

Howat, I. M., I. Joughin, and T. A. Scambos (2007), Rapid changes in ice discharge from Greenland outlet glaciers, *Science*, *315*(5818), 1559–1561, doi:10.1126/science.1138478.

Jackson, R. H., F. Straneo, and D. A. Sutherland (2014), Externally forced fluctuations in ocean temperature at Greenland glaciers in non-summer months, *Nat. Geosci.*, *7*(7), 503–508.
Klinck, J. M., J. J. O'Brien, and H. Svendsen (1981), A simple model of fjord and coastal circulation interaction, *J. Phys. Oceanogr.*, *11*(12), 1612–1626, doi:10.1175/1520-0485(1981)011<1612:ASMOFA>2.0.CO;2.
Kwok, R., G. F. Cunningham, and S. S. Pang (2004), Fram Strait sea ice outflow, *J. Geophys. Res.*, *109*, C01009, doi:10.1029/2003JC001785.
Lentz, S. J., and J. Largier (2006), The influence of wind forcing on the Chesapeake Bay buoyant coastal current, *J. Phys. Oceanogr.*, *36*(7), 1305–1316, doi:10.1175/JPO2909.1.
Moon, T., I. Joughin, B. Smith, and I. Howat (2012), 21st-Century Evolution of Greenland Outlet Glacier Velocities, *Science*, *336*(6081), 576–578, doi:10.1126/science.1219985.
Moore, G. W. K., and I. A. Renfrew (2005), Tip jets and barrier winds: A QuikSCAT climatology of high wind speed events around Greenland, *J. Clim.*, *18*(18), 3713–3725, doi:10.1175/JCLI3455.1.
Murray, T., et al. (2010), Ocean regulation hypothesis for glacier dynamics in southeast Greenland and implications for ice sheet mass changes, *J. Geophys. Res.*, *115*, F03026, doi:10.1029/2009JF001522.
Myers, P. G., N. Kulan, and M. H. Ribergaard (2007), Irminger Water variability in the West Greenland Current, *Geophys. Res. Lett.*, *34*, L17601, doi:10.1029/2007GL030419.
Nilsen, F., F. Cottier, R. Skogseth, and S. Mattsson (2008), Fjord-shelf exchanges controlled by ice and brine production: The interannual variation of Atlantic Water in Isfjorden, Svalbard, *Cont. Shelf Res.*, *28*(14), 1838–1853, doi:10.1016/j.csr.2008.04.015.
Oltmanns, M., F. Straneo, G. W. K. Moore, and S. H. Mernild (2014), Strong Downslope Wind Events in Ammassalik, Southeast Greenland, *J. Clim.*, *27*(3), 977–993, doi:10.1175/JCLI-D-13-00067.1.
Outten, S. D., I. A. Renfrew, and G. N. Petersen (2009), An easterly tip jet off Cape Farewell, Greenland. II: Simulations and dynamics, *Q. J. R. Meteorol. Soc.*, *135*(645), 1934–1949, doi:10.1002/qj.531.
Padman, L., and S. Erofeeva (2004), A barotropic inverse tidal model for the Arctic Ocean, *Geophys. Res. Lett.*, *31*, L02303, doi:10.1029/2003GL019003.
Pawlowicz, R., B. Beardsley, and S. Lentz (2002), Classical tidal harmonic analysis including error estimates in MATLAB using T_TIDE, *Comput. Geosci.*, *28*(8), 929–937, doi:10.1016/S0098-3004(02)00013-4.
Pickart, R. S., D. J. Torres, and P. S. Fratantoni (2005), The East Greenland Spill Jet, *J. Phys. Oceanogr.*, *35*(6), 1037–1053, doi:10.1175/JPO2734.1.
Rudels, B., E. Fahrbach, J. Meincke, G. Budéus, and P. Eriksson (2002), The East Greenland Current and its contribution to the Denmark Strait overflow, *J. Mar. Sci.*, *59*, 1133–1154, doi:10.1006/jmsc.2002.1284.
Schjøth, F., C. S. Andresen, F. Straneo, T. Murray, K. Scharrer, and A. Korablev (2012), Campaign to map the bathymetry of a major Greenland fjord, *Eos Trans. AGU*, *93*(14), 141–142, doi:10.1029/2012EO140001.
Schulze, L. M., and R. S. Pickart (2012), Seasonal variation of upwelling in the Alaskan Beaufort Sea: Impact of sea ice cover, *J. Geophys. Res.*, *117*, C06022, doi:10.1029/2012JC007985.
Stearns, L. A., and G. S. Hamilton (2007), Rapid volume loss from two East Greenland outlet glaciers quantified using repeat stereo satellite imagery, *Geophys. Res. Lett.*, *34*, L05503, doi:10.1029/2006GL028982.
Stigebrandt, A. (1990), On the response of the horizontal mean vertical density distribution in a fjord to low-frequency density fluctuations in the coastal water, *Tellus, Ser. A*, *42*(5), 605–614, doi:10.1034/j.1600-0870.1990.t01-1-00010.x.
Straneo, F., and P. Heimbach (2013), North Atlantic warming and the retreat of Greenland's outlet glaciers, *Nature*, *504*(7478), 36–43, doi:10.1038/nature12854.
Straneo, F., G. S. Hamilton, D. A. Sutherland, L. A. Stearns, F. Davidson, M. O. Hammill, G. B. Stenson, and A. Rosing-Asvid (2010), Rapid circulation of warm subtropical waters in a major glacial fjord in East Greenland, *Nat. Geosci.*, *3*(3), 182–186, doi:10.1038/ngeo764.
Straneo, F., D. A. Sutherland, D. Holland, C. Gladish, G. S. Hamilton, H. L. Johnson, E. Rignot, Y. Xu, and M. Koppes (2012), Characteristics of ocean waters reaching Greenland's glaciers, *Ann. Glaciol.*, *53*(60), 202–210, doi:10.3189/2012AoG60A059.
Sutherland, D. A. (2008), The East Greenland Coastal Current: Its structure, variability, and large-scale impact, PhD thesis, MIT, Cambridge, Mass.
Sutherland, D. A., and R. S. Pickart (2008), The East Greenland Coastal Current: Structure, variability, and forcing, *Prog. Oceanogr.*, *78*(1), 58–77, doi:10.1016/j.pocean.2007.09.006.
Sutherland, D. A., R. S. Pickart, E. Peter Jones, K. Azetsu-Scott, A. Jane Eert, and J. Ólafsson (2009), Freshwater composition of the waters off southeast Greenland and their link to the Arctic Ocean, *J. Geophys. Res.*, *114*, C05020, doi:10.1029/2008JC004808.
Sutherland, D. A., F. Straneo, G. B. Stenson, F. J. M. Davidson, M. O. Hammill, and A. Rosing-Asvid (2013), Atlantic water variability on the se Greenland continental shelf and its relationship to SST and bathymetry, *J. Geophys. Res. Oceans*, *118*, 847–855, doi:10.1029/2012JC008354.
Thierry, V., E. de Boisséson, and H. Mercier (2008), Interannual variability of the Subpolar Mode Water properties over the Reykjanes Ridge during 1990–2006, *J. Geophys. Res.*, *113*, C04016, doi:10.1029/2007JC004443.
Velicogna, I. (2009), Increasing rates of ice mass loss from the Greenland and Antarctic ice sheets revealed by GRACE, *Geophys. Res. Lett.*, *36*, L19503, doi:10.1029/2009GL040222.
Vieli, A., and F. Nick (2011), Understanding and modelling rapid dynamic changes of tidewater outlet glaciers: Issues and implications, *Surv. Geophys.*, *32*(4-5), 437–458, doi:10.1007/s10712-011-9132-4.
Wilkinson, D., and S. Bacon (2005), The spatial and temporal variability of the East Greenland Coastal Current from historic data, *Geophys. Res. Lett.*, *32*, L24618, doi:10.1029/2005GL024232.
Williams, W. J., E. C. Carmack, K. Shimada, H. Melling, K. Aagaard, R. W. Macdonald, and R. Grant Ingram (2006), Joint effects of wind and ice motion in forcing upwelling in Mackenzie Trough, Beaufort Sea, *Cont. Shelf Res.*, *26*(19), 2352–2366, doi:10.1016/j.csr.2006.06.012.